CHEMISTRY
A European Journal

A Journal of
ChemPubSoc Europe

Accepted Article

Title: Single oxidative collision events of silver nanoparticles: understanding the rate-determining chemistry

Authors: Kamonwad Ngamchuea, Richard O. D. Clark, Stanislav V. Sokolov, Neil P. Young, Christopher Batchelor-McAuley, and Richard G. Compton

This manuscript has been accepted after peer review and appears as an Accepted Article online prior to editing, proofing, and formal publication of the final Version of Record (VoR). This work is currently citable by using the Digital Object Identifier (DOI) given below. The VoR will be published online in Early View as soon as possible and may be different to this Accepted Article as a result of editing. Readers should obtain the VoR from the journal website shown below when it is published to ensure accuracy of information. The authors are responsible for the content of this Accepted Article.

To be cited as: *Chem. Eur. J.* 10.1002/chem.201703591

Link to VoR: http://dx.doi.org/10.1002/chem.201703591

Supported by
ACES

WILEY-VCH

10.1002/chem.201703591

Single oxidative collision events of silver nanoparticles: understanding the rate-determining chemistry

Kamonwad Ngamchuea, Richard O. D. Clark, Stanislav V. Sokolov, Neil P. Young, Christopher Batchelor-McAuley,* Richard G. Compton*

* corresponding authors: Christopher Batchelor-McAuley and Richard G. Compton, Department of Chemistry, Physical & Theoretical Chemistry Laboratory, University of Oxford, South Parks Road, Oxford, OX1 3QZ, United Kingdom

Emails: christopher.batchelor-mcauley@chem.ox.ac.uk, richard.compton@chem.ox.ac.uk.

Tel: +44(0)1865275 957 Fax: +44(0)1865275410

Abstract

The oxidative dissolution of citrate-capped silver nanoparticles (AgNPs) is investigated herein by two electrochemical techniques: nano-impacts and anodic stripping voltammetry. *Nano-impacts* or single nanoparticle-electrode collisions allow the detection of *individual* nanoparticles. The technique offers an advantage over surface-immobilized methods such as anodic stripping voltammetry as it eliminates the effects of particle agglomeration/ aggregation. The electrochemical studies are performed in different electrolytes (KNO_3, KCl, KBr and KI) at varied concentrations (≤ 20 mM). In nano-impact measurements, the AgNP undergoes *complete* oxidation upon impact at a suitably potentiostated electrode. The frequency of the nanoparticle-electrode collisions observed as current-transient spikes depends on the electrolyte identity, its concentration and the potential applied at the working electrode. The frequencies of the spikes are significantly higher in the presence of halide ions and increase with increasing potentials. From the frequency, the rate of AgNP oxidation as compared with the timescale the AgNP is in electrical contact with the electrode can be inferred, and hence is indicative of the relative kinetics of the oxidation process. Primarily based on these results, we propose the initial formation of the silver (I) nucleus (Ag^+, AgCl, AgBr or AgI) as the rate-determining process of silver oxidation on the nanoparticle.

This article is protected by copyright. All rights reserved.

Accepted Manuscript

1 Introduction

The use of electrochemical techniques to determine the concentrations, volumes and surface areas of nanoparticles has been widely reported in literature.[1] Among these, anodic stripping voltammetry[2] is one of the most widely-used methods. Anodic stripping voltammetry has also been used in the characterization of core-shell[3] and alloy nanoparticles,[4] the determination of the surface energy of single nanoparticles[5] and the extent of nanoparticles agglomeration.[6] There are however limitations to this technique arising from agglomeration/aggregation of the nanoparticles on the electrode surface upon the evaporation of solvent and a variation of the possible diffusion regimes.[6-7] In addition, the peak height and peak position alter in the presence of different capping agents,[8] electrolytes,[9] nanoparticle surface coverage and the size of the nanoparticle itself.[7b, 10]

As an alternative to stripping voltammetry, single nanoparticle collisions or the 'nano-impact' technique can be used in the detection of *individual* nanoparticles.[11] Nano-impacts have been utilized in extensive applications such as the detection of femtomolar levels of nanoparticles[12] and the investigations of nanoparticle catalytic activity.[13] Upon impact (collision) with a suitably potentiostated electrode, the redox-active nanoparticles may be oxidized or reduced, resulting in current-transient spikes.[14] Knowledge of how this processes varies as a function of potential can under suitable conditions and upon assumption of a mechanism allow the kinetics of the nano-redox event to be inferred.[15] For an ideal system of nanoparticles diffusing freely in the solution, a number of studies have discussed the relations between the *frequency* of the spikes,[11a] the first passage time of the impact[16] and the concentration of the nanoparticles in the suspension. In practice, however, the observed spike frequency can be markedly influenced by the electrolyte used.[17]

This work studies the oxidative dissolution events of citrate-capped silver nanoparticles (AgNPs). AgNPs are extensively used in commercial products from textiles to antimicrobial and biomedical applications. A large quantity of AgNPs are released into the environment and there are concerns about health risks and environmental damage.[18] Electrochemical methods provide simple, quick and easy measurements of the AgNPs' sizes and concentrations. However, due to the issues raised above regarding the variation in the amperometric responses in different media, it is essential to understand the fundamental/physical mechanisms of the AgNPs oxidation that takes place at the electrode

This article is protected by copyright. All rights reserved.

Accepted Manuscript

interface. The electrochemical response of AgNPs oxidation is studied herein using the novel nano-impact technique along with anodic stripping voltammetry. With the aim of understanding the rate-determining process of the AgNPs oxidation, the effects of the electrolytes (KNO_3, KCl, KBr and KI) and their concentrations on the stripping voltammograms and nano-impacts spikes are investigated. From this study, we gain physical insight into the initiation and the rate-determining process of the AgNPs oxidation at the electrode surface.

In the nano-impact measurements, the total charge transferred during each current-transient spike directly relates to the *number* of constituent electroactive atoms or molecules of the nanoparticles, irrespective of their shape[19] or the presence of capping agents.[8] This is different from other techniques that measure the length scale of the particles such as transmission electron microscopy (TEM). In the comparison of the sizes determined using TEM to that obtained from electrochemical measurements, careful inference of the particle volume from the two-dimensional TEM images is emphasized in this work. In particular, consideration of the particle shape is taken into account as (large) metal nanoparticles exhibit a significant extent of faceting.[20] From the careful analysis of 180 TEM images and over 5,000 spikes, we provide evidences for the *complete* oxidation of the AgNPs upon the impact at a suitably potentiostated electrode although the frequency of the nano-impact spikes is *lower* than the predicted diffusion-limited fluxes.

2 Experimental

2.1 Chemical reagents

Spherical 50 nm diameter citrate-AgNPs (NanoXact, 0.02 mg/mL silver, 2 mM sodium citrate) were obtained from Nanocomposix, USA. All other reagents were purchased from Sigma-Aldrich and used as received without further purification: potassium nitrate (≥99.0%), potassium chloride (≥99.5%), potassium bromide (≥99.0%) and potassium iodide (≥99.5%). All solutions were prepared using deionized water (Millipore) with a resistivity of 18.2 MΩ cm at 25°C.

This article is protected by copyright. All rights reserved.

Accepted Manuscript

2.2 Sizing of the AgNPs

Transmission electron microscopy (TEM, 300 kV JEOL 3000F microscope) was used to determine the size of the AgNPs, detailed in Section S1 (SI).

2.3 Stability of the AgNPs in different electrolytes

The stabilities of AgNPs in 20 mM KNO_3, KCl, KBr or KI electrolyte solutions were studied via UV-Vis measurements (λ = 250 – 800 nm) with a Shimadzu UV-1800 spectrophotometer in disposable cuvettes (Eppendorf UVette, Sigma-Aldrich) using a 10 mm optical path length.

2.4 Anodic stripping voltammetry

Anodic stripping experiments were performed with a µAutolab Type III potentiostat (Utrecht) using a glassy carbon working electrode (3 mm diameter, BASi, USA) and a platinum mesh counter electrode. A leakless Ag/AgCl (in 3.4 M KCl, eDAQ) or a saturated calomel electrode (BASi, USA) was used as a reference electrode.

Prior to use, the glassy carbon electrode was polished to a mirror finish using a water-alumina slurry (1.0 µm, 0.3 µm and 0.05 µm; Buehler, USA) on soft lapping pads (Buehler, USA). A 5 µL aliquot of the 48.2 pM AgNPs suspension was then dropcast onto the surface of the glassy carbon electrode and allowed to dry under a flowing nitrogen atmosphere. The AgNP-modified glassy carbon electrode was transferred to the electrolyte solution under studies (KNO_3, KCl, KBr or KI). The system was then subjected to cyclic voltammetric measurements initially scanning anodically in the potential range of -0.4 V to 1.2 V vs. SCE at the scan rate of 10 mV s^{-1}.

2.5 Nano-impacts

Nano-impact experiments were performed with a low noise potentiostat that was built in-house. The details of the potentiostat have been described in full elsewhere.[21] The analog signal was filtered using two cascaded RC filters (100Hz). This signal was digitized at a rate of 50k Hz and subsequently digitally filtered using a four-pole Bessel filter (100 Hz), as implemented by the Python SciPy library. Bessel filters have been demonstrated to conserve the total charge transferred in an impact event.[22] A carbon microdisc (33 µm diameter, IJ Cambria Scientific Ltd, UK) and a platinum mesh were used as working and counter

This article is protected by copyright. All rights reserved.

Accepted Manuscript

electrodes respectively. A leakless Ag/AgCl (in 3.4 M KCl, eDAQ) or a saturated calomel electrode (BASi, USA) was used as a reference electrode.

Cyclic voltammetric measurements initially scanning anodically in the potential range of -0.4 V to 1.2 V vs. SCE at the scan rate of 10 mV s^{-1} were performed in the solutions containing 12 pM AgNPs and varied supporting electrolytes (KNO_3, KCl, KBr and KI). A 16-bit DAC was used to provide the waveform with a full potentiostat range of ±2 V (effective staircase voltammetry step size of 61 μV)

Note that the anodic stripping voltammetry and nano-impact measurements in all KNO_3 and in KCl solutions at and below 5 mM concentrations are performed against a leakless Ag/AgCl reference electrode (E = -0.039 V vs. SCE) to prevent the contamination of Cl^-, which would affect the position of the anodic stripping voltammetry (Section S2 in the SI). Otherwise, the voltammetric measurement is performed against a standard calomel reference electrode (SCE). All the results below are presented as *vs. SCE* for clear comparison.

3 Results

The AgNPs are first characterized using transmission electron microscope (TEM), where the inference of the nanoparticle's volume from the two-dimensional TEM images is discussed in detail (Section 3.1). Next, the stability of the AgNPs in different electrolyte solutions is demonstrated by UV-Vis measurements as a function of time (Section 3.2). The oxidation of AgNPs is then studied using anodic stripping voltammetry and the nano-impact method. The factors influencing the resulting electrochemical responses are investigated, in particular the effects of the electrolyte concentrations (Section 3.3) and the presence of different anions (Section 3.4).

3.1 TEM analysis of AgNPs

The commercial spherical citrate-capped AgNPs were characterized by transmission electron microscope (TEM). It was observed that although described as spherical, the shapes of the AgNPs are not that of a perfect sphere. In other words, the circularity of the two-dimensional images is less than unity. Examples of the resulting images are provided in Section S1 (SI). This is true not only this batch of commercial AgNPs, the citrate-capped AgNPs employed in other electrochemical studies, but both home-made via citrate reduction and commercial products from different sources, show a significant level of non-sphericity,[23] due to the

This article is protected by copyright. All rights reserved.

Accepted Manuscript

presence of various facets.[20] As the particles are not perfect spheres, there is ambiguity in the determination of the particle 'radius'. Notably, any inaccuracy in the radius measurement gives rise to a significantly large error in volume, as the volume scales with r^3. Importantly, in terms of comparison with the experimental nano-impact electrochemical data, it is the volume rather than the length scale that is required.

In order to estimate the volume of the AgNPs more accurately, the resulting two-dimensional TEM images of AgNPs are classified into circular (Figure 1b), hexagonal (Figure 1c) and 'other' ambiguous shapes (Figure 1d). However, we comment that the circularity of a particle 2D projection in an image is generally a poor indicator of a particle's inscribed volume compared to that of a sphere. From the analysis of 180 nanoparticles, it was found for this sample that the particles are approximately equally distributed between the three classes of particle shapes. It is approximated that circular and hexagonal images correspond to spherical and icosahedral particles respectively.[23d] For hexagonal images, all three diagonals are measured and the average is taken as the diameter of the circumscribed sphere. In the case of nanoparticles with ambiguous shapes, the maximal diameter is used to describe the circumscribed sphere. The circumscribed volume is determined and the actual volume of the nanoparticles (V_{NP}) of the different shapes is calculated according to the following equation:

$$V_{\mathrm{NP}} = \frac{4\pi R_{\mathrm{c}}^3}{3} \times f \qquad (1),$$

where R_{c} is the radius of the sphere circumscribing the nanoparticle. f is a correction factor accounting for the overestimation of the nanoparticle volume from the radius of the circumscribed sphere.

The values of f are 1 and 0.605 for spherical and icosahedral nanoparticles respectively.[23d] In the case of nanoparticles with ambiguous shapes, the f-factor is likely to be much smaller than 0.605 of the highly symmetric icosahedron and is chosen semi-arbitrarily to be 0.5 in the present work. This value of 0.5 is relatively conservative given the distinct non-sphericity of some of the particles imaged. The actual f value depends on the exact shapes of the nanoparticles and cannot be determined from the two-dimensional images alone. Figure S2 (SI) displays the size distribution of the AgNPs using the f-factors in the range of 0.3 - 0.5.

In the following sections, the TEM sizes are compared with the volumes determined via nano-impact measurements. Accordingly, the size of the AgNPs as measured from the TEM

This article is protected by copyright. All rights reserved.

Accepted Manuscript

data is thus converted via Faradays first law and presented in term of an *equivalent* total *charge* (Q_{equiv}). In the case that the entire AgNP is oxidized, the charge transferred per nanoparticle (Q_{NP}) can be calculated according to:

$$Q_{NP} = \frac{\rho z F}{A_r} V_{NP} \quad (2),$$

where z is the number of electrons transferred per atom. z = 1 for silver oxidation. F is the Faraday constant (96,485 C mol^{-1}). A_r is the atomic mass of silver (107.9 g mol^{-1}) and ρ is the density of silver (10.5×10^6 g m^{-3}).[24]

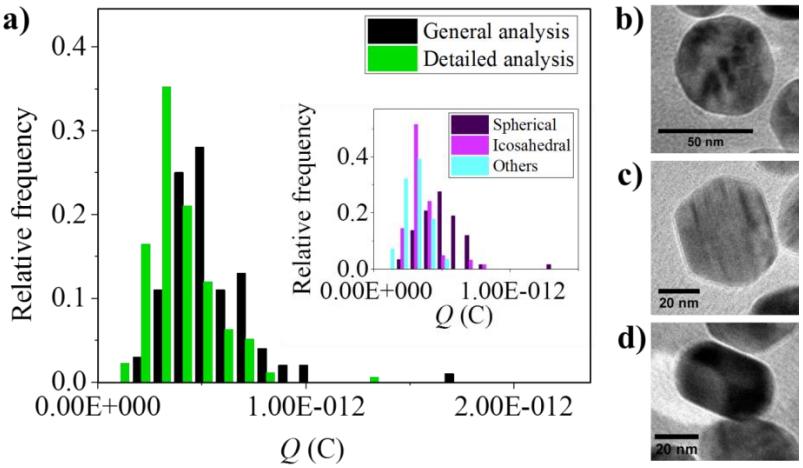

Figure 1: **a)** A histogram showing the size distribution (presented as charges (*Qequiv*); see eqn. 2) of AgNPs determined by TEM and analyzed using two different approaches: 'general analysis' and 'detailed analysis' as explained in the text. Examples of **b)** spherical, **c)** icosahedral and **d)** ambiguous shapes of AgNPs. More examples of TEM images are provided in Section S1 (SI).

Figure 1a presents the size distribution of the AgNPs as estimated from the TEM images and presented in terms of the expected *equivalent* charges as analyzed by two different approaches. First is the 'general analysis' where no correction is made to account for the irregularity of the nanoparticles. Second is the 'detailed analysis' where the AgNPs are characterized into spherical (f = 1), icosahedral (f = 0.605) and other ambiguous shapes (f = 0.5). The size distributions of the different shapes are presented in the inlay in Figure 1a. Compared with the detailed analysis (Q_{equiv} = $3.9 \times 10^{-13} \pm 1.6 \times 10^{-13}$ C, corresponds to equivalent spherical radii of 21 ± 3 nm), the charges are more biased to higher values when using the general analysis (Q_{equiv} = $5.3 \times 10^{-13} \pm 2.1 \times 10^{-13}$ C, corresponds to spherical radii

This article is protected by copyright. All rights reserved.

Accepted Manuscript

of 24 ± 3 nm, corresponding in this to ~30% discrepancy in charges). This discrepancy arises due to the overestimation of the volume of the non-spherical particles. The importance of detailed analysis of the size of the AgNPs will be further highlighted in Section 3.4.2 where we compare the charges of the AgNPs oxidation upon impact at the electrode to the sizes characterized by TEM.

3.2 Stability of the AgNPs in different electrolytes

Repeated UV-Visible spectra were recorded over 20 min after the suspensions of 12 pM AgNPs were mixed with 20 mM of KNO_3, KCl, KBr or KI electrolytes. The resulting spectra are displayed in Section S3 (SI). Silver nanoparticle suspensions exhibit a strong plasmonic peak at ~400 nm. The peak's exact position, shape and magnitude are sensitive to not only the nanoparticles size and geometry but also their local environment.[25] Consequently, this peak can be used to monitor the nanoparticle suspensions stability. In all the electrolytes studied, the wavelength at maximum absorbance (λ_{max}) of the AgNPs is 423.3±0.7 nm and the magnitude of maximum absorbance (Abs_{max}) remained constant throughout the 20 min studied. This evidenced the stability of the particles under these ionic conditions.

3.3 AgNPs oxidation: the effects of the electrolyte concentrations

In this section, we focus on the effect of the electrolyte concentrations (≤ 20 mM) towards the amperometric responses of AgNPs oxidation. Two electrolytes KNO_3 and KCl are studied. The AgNPs oxidation events are first studied using anodic stripping voltammetry, then second by the nano-impact technique.

3.3.1 Anodic stripping voltammetry

AgNPs were first immobilized on the surface of glassy carbon electrode by dropcasting 2.4×10^{-16} moles of the AgNPs (7.8×10^{-10} moles of Ag atoms) on a 3 mm diameter electrode, yielding a surface coverage of ca. 4.5% by area. The glassy carbon electrode modified with the AgNPs was then subjected to cyclic voltammetry measurement in KNO_3 or KCl electrolytes of varied concentrations (0-20 mM).

Figure 2 displays the anodic stripping voltammograms of AgNPs in the different concentrations of electrolytes studied. In the absence of added electrolyte, the stripping

This article is protected by copyright. All rights reserved.

Accepted Manuscript

voltammogram shows a broad anodic peak at 0.57 V vs. SCE. In KNO_3 solutions, the oxidative stripping takes place at 0.38 ± 0.07 V vs. SCE for all the concentrations studied. The anodic stripping of AgNPs in KCl solutions occurs at 0.21, 0.17, 0.14 and 0.11 V vs. SCE for 1, 5, 10 and 20 mM KCl respectively. The plot of the peak potential (E_p) against $\log_{10}([Cl^-])$ gives a slope of 76 ± 8 mV, the value of which is discussed below. Note that the stripping in KCl occurs at less positive potentials than in KNO_3 and the potential is further lowered with increasing concentrations of Cl^-.

In comparing the two responses, given that the quantity of the AgNPs immobilized on the electrode surface is the same, the extent of agglomeration/aggregation and the diffusion regimes can be inferred to be comparable.[6] In addition, both KCl and KNO_3 have the same ionic strength at equal concentrations. Hence, the difference in the measured peak potentials arises from the influence of the anions. In KNO_3 solution and in the absence of any complexing agents, the AgNPs are oxidized to Ag^+. On the other hand, the products of silver oxidation in the presence of Cl^- ions are likely AgCl(s) or at higher chloride complexes such as $AgCl_2^-$.[26] For an oxidation involving one Cl^- ion per Ag atom, a shift in the anodic stripping peak of 59 mV per a unit of $\log_{10}([Cl^-])$ is expected according to the Nernst equation.[27] The plot of the anodic peak potentials (E_p) against $\log_{10}([Cl^-])$ however gives a slope of 76 ± 8 mV. This may be evidence for the participation of more than one Cl^- ions per Ag atom, and thus suggests the (partial) formation of $AgCl_2^-$ and other higher halide complexes. The standard electrode potential of Ag(s)/Ag^+(aq) and Ag(s)/AgCl(s) are 0.80 and 0.22 V vs. SHE respectively.[28] The negative shifts in the stripping peak potential in the presence of chloride predominantly reflects the more thermodynamically favourable oxidation of AgNPs in KCl than KNO_3, and more so at higher concentrations of Cl^-.

The amount of charge transferred during oxidation of the large ensemble of nanoparticles in all electrolytes are of similar order of $1.6\times10^{-5} \pm 4.8\times10^{-6}$ C, corresponding to 22 ± 6 % of the immobilized AgNPs being oxidized. The incomplete oxidation is likely a result of the particles agglomeration/aggregation on the electrode surface as arising from nanoparticle/electrode connectivity issues.[7a] Previous experimental work utilising gold-silver contacts has evidenced the presence of poor electrical contact between nanoparticles in an agglomerate.[29] For the same coverage of AgNPs immobilized on the electrode surface, the oxidation of AgNPs in the presence of Cl^- ions gives rise to a much sharper anodic stripping peak than in KNO_3 or deionized water (Figure 2). To further investigate the

This article is protected by copyright. All rights reserved.

Accepted Manuscript

difference of AgNP oxidation in KNO_3 and KCl, the oxidative dissolution of *individual* AgNP is studied next using the nano-impact technique.

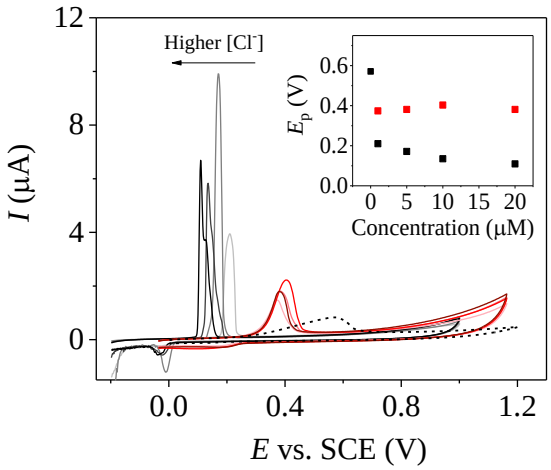

Figure 2: Anodic stripping voltammograms of 2.4×10^{-16} moles of AgNPs dropcasted on a 3 mm diameter glassy carbon electrode (surface coverage of 4.5%) in deionized water (dashed line), 1, 5, 10 and 20 mM KNO_3 (pale pink → dark red), and 1, 5, 10 and 20 mM KCl (grey → black). The inlay shows the plot of the position of the anodic stripping peaks (E_p) as a function of electrolyte concentrations.

3.3.2 Nano-impacts: single nanoparticle-electrode collisions

The oxidation of AgNPs is next studied via nano-impact technique.[11a] In contrast to anodic stripping voltammetry, nano-impacts allow the detection of individual nanoparticles, eliminating the complication that may arise from different diffusion regimes or particle aggregation/agglomeration on the electrode surface.[6]

In the literature a number of works have sought to look at the potential dependency of a nano-impact event, focusing on both destructive [15b, 17] and mediated processes[30], where the influence of the electrode potential upon the observed impact frequency has also been highlighted.[17, 30b] However, with only a few notable exceptions[31] these works typically involve nano-impact studies performed using chronoamperometry at a series of fixed potentials, in the present work cyclic voltammetry is employed to study the effect of the applied potentials simultaneously with obtaining nanoparticle size information (as derived from the total charge under a spike) and impact frequency of the particles in a single measurement.

This article is protected by copyright. All rights reserved.

Accepted Manuscript

10.1002/chem.201703591

The suspensions of 12 pM AgNPs in 0, 1, 5 or 20 mM of KNO_3 or KCl were subjected to cyclic voltammetry measurements at a carbon microdisc electrode at the scan rate of 10 mV s^{-1}. Figure 3 presents the representative cyclic voltammograms showing nano-impact spikes of AgNPs oxidation in 1, 5 and 20 mM KCl (Figures 3a-c), and 1, 5 and 20 mM KNO_3 (Figures 3d-f). The nano-impact results in zero added electrolyte are presented in Figure S5 (SI). Inlayed in Figures 3 a-f are images showing the representative spikes shapes for the oxidative events, the duration of these feature is 10-20 ms. However, this timescale reflects the speed of the used electronics and not the course of the nano-impact event at the interface. In the present study the focus of the work is to determine the magnitude (charge) of the individual impact events and not the structure of the spike itself. Consequently, this work utilises relatively slow low-pass filtering (100 Hz) where the filter and amplifier conserve the charge passed, this ensures as large as feasible signal-to-noise ratio is attained for the present electrode setup. We comment that the motion of nanoparticles adjacent to an electrode[30a, 32] is likely an important aspect of the oxidation event [23a, b, 33]; however, this process occurs on a timescale which is significantly shorter than is studied in the present work.

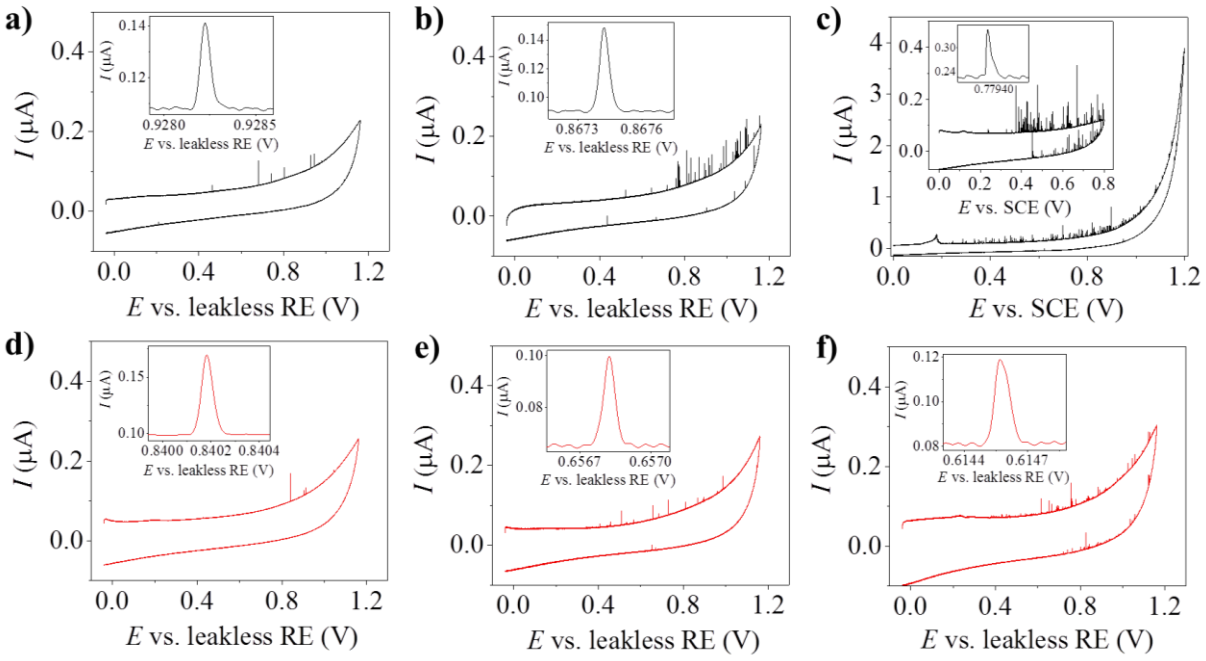

Figure 3: Representative cyclic voltammograms showing nano-impact spikes of 12 pM AgNPs in **a)** 1 mM KCl, **b)** 5 mM KCl, **c)** 20 mM KCl, **d)** 1 mM KNO_3, **e)** 5 mM KNO_3 and **f)** 20 mM KNO_3. Carbon microdisc (20.5 μm diameter) working electrode. Scan rate of 10 mV s^{-1}.

Without added electrolyte, no oxidative spikes are observed although we note the solution contains ~0.5 mM of citrate from the AgNP stock solution. From the previous section, we

This article is protected by copyright. All rights reserved.

Accepted Manuscript

have shown that AgNPs can be oxidized in the absence of electrolyte with the peak potential at 0.57 V vs. SCE. The fact that no spikes are observed suggests that the oxidation of any impacting AgNPs in the absence of electrolyte is very slow as compared to the time the AgNPs are in electrical contact with the electrode.

In the presence of added supporting electrolyte, nano-impact spikes are observed at potentials more positive than the stripping potentials of AgNPs in the relevant electrolytes. In order to investigate the effect of the applied potentials on the size and frequency of the nano-impact spikes, the resulting voltammograms were sub-divided into smaller potential ranges of 0.1 V intervals. However, we comment that this analysis is restricted to the measurement of spikes observed in the forward scan. The use of higher electrode potentials can result in a decrease in the observed impact frequency. This influence can be seen from comparing the nano-impact spikes of AgNPs in 20 mM KCl subjected to the maximum potentials of 1.2 V (Figure 3c) and 0.8 V vs. SCE (Inlay in Figure 3c). No spikes are observed in the backward cathodic scan of the former while the latter shows a significant number of features. This suggests that at very high potentials, reactive (possibly radical, peroxide or O_2/H^+) [34] species that can oxidize the AgNPs within the diffusion layers may be formed. On the assumption that a steady-state diffusion layer forms at the electrode surface during solvent breakdown then for the given size and with the passage of 4nA of current, at the electrode the surface concentration of oxygen is predicted to be ~60uM and the local pH will be approximately 4.3 (assuming the oxidative process to be the full four electron oxidation of water). The total silver atom concentration used in these experiments is ~25 uM (12pM AgNps with an average of ~$2x10^6$ silver atoms per particle). Hence, the oxidation of the silver nanoparticles by the products of solvent breakdown in the vicinity of the electrode is likely favourable. Hence, due to this influence of solvent breakdown upon the nanoparticle oxidation process, only the spikes observed in the forward scans are considered for analysis.

The area under each spike relates to the amount of charge transferred during a single nanoparticle oxidation event. At all potentials higher than the stripping potential, the average measured charges are in excellent agreement with the size (volume) determined using transmission electron microscope; see Figure 4a. This implies that if a nano-impact event occurs at a sufficiently biased electrode then the oxidation of the individual AgNP goes to completion. The evidence of the *complete* dissolution of the AgNPs is further provided and discussed in detail towards the end of Section 3.4.2.

This article is protected by copyright. All rights reserved.

Accepted Manuscript

10.1002/chem.201703591

In addition to the size of the nanoparticles, the frequency of the spikes (the number of spikes per second) is analyzed for each of the 0.1 V potential intervals (equivalent to 10 s at the scan rate of 10 mV s^{-1}). Figure 4b presents the frequency of the nano-impact spikes taking place in 5 and 20 mM of KNO_3 or KCl as a function of applied potentials. Note that at 1 mM, the frequencies are significantly lower than at 5 and 20 mM of the same electrolytes and very low such that no statistically relevant information can be extracted.

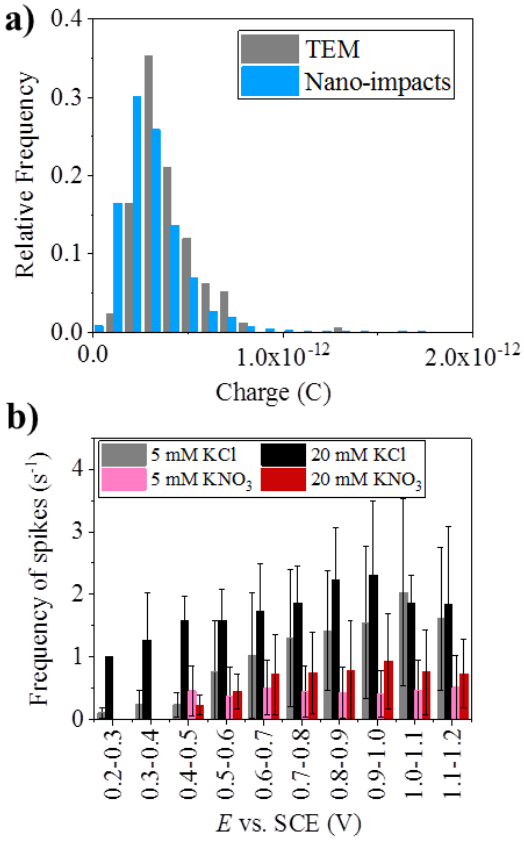

Figure 4: **a)** The histograms display the distribution of AgNPs sizes calculated from the charge transfer of nano-impact spikes in 5 mM and 20 mM KNO_3 and KCl, compared with the sizes determined by TEM. **b)** The bar graph showing the frequency of nano-impact spikes of 12 pM AgNPs oxidation events in 5 mM and 20 mM KNO_3 and KCl electrolyte solutions.

The frequency of the nanoparticle-electrode collisions increases with increasing potentials. Furthermore, at both 5 mM and 20 mM, the frequency in KCl is significantly (by up to a factor of 7) higher than in KNO_3, this is in agreement with reports by Krause et al.[17] from chronoamperometric results. The increase in frequency with the applied potentials and the higher frequencies in KCl than in KNO_3 may arise from either the difference in the mass-transport flux of AgNPs to the electrode or the rate of the AgNPs oxidation at the electrode. The former is not feasible and will be discussed in detail in Section 4. The latter can be

This article is protected by copyright. All rights reserved.

Accepted Manuscript

limited by a number of factors and full insight cannot be deduced from this result alone. In the next section, we will further investigate the roles of Cl^- and other halide ions in the rate-determining step.

3.4 AgNPs oxidation: the effect of the electrolyte anion identity

In the previous section, it was observed that there is a substantial difference in the frequency of nano-impact spikes with the use of either KCl or KNO_3 as the supporting electrolyte, thus suggesting the important role of Cl^- in the rate-determining process of AgNPs oxidation. In this section, Br^- and I^- are further investigated in comparison to Cl^-. The AgNPs are first subjected to anodic stripping voltammetry to study the effect of the anions towards the stripping potential of AgNP oxidation. Nano-impacts are then performed to investigate the oxidation process at a single nanoparticle scale.

3.4.1 Anodic stripping voltammetry

The glassy carbon electrode modified with AgNPs as already described in Section 3.3.1 was subjected to cyclic voltammetric measurements in 20 mM of KNO_3, KCl, KBr or KI. Figure 5 displays the anodic stripping voltammograms of AgNPs in the different electrolytes studied. The positions of the oxidative peaks are 0.37, 0.11, -0.02 and -0.24 V vs. SCE for KNO_3, KCl, KBr and KI respectively. The more negative peak potential of KI as compared to other electrolytes implies the relative 'ease' (see below) of silver oxidation in the presence of I^-.

For all the electrolytes studied herein, the difference in the standard reaction Gibbs energy (ΔG_r^0) of the AgNPs oxidation is a result of the formation of the different oxidation products, see below.

$$Ag(s) + X^-(aq) \xrightarrow{\triangle G_r^0} e^- + AgX(s) \quad (3),$$

$$Ag(s) \xrightarrow{\triangle G_1^0} e^- + Ag^+(aq) \quad (4),$$

$$Ag^+(aq) + X^-(aq) \underset{}{\overset{\triangle G_2^0}{\rightleftharpoons}} AgX(s) \quad (5),$$

$$\Delta G_r^0 = \Delta G_1^0 + \Delta G_2^0 \quad (6),$$

This article is protected by copyright. All rights reserved.

Accepted Manuscript

$$\Delta G_2^0 = -RT \ln(K_{sp}) \quad (7),$$

where R and T are the molar gas constant (8.314 J mol^{-1} K^{-1}) and absolute temperature respectively. K_{sp} is the solubility product constant. For AgCl, AgBr and AgI in aqueous solutions at 25°C under atmospheric pressure, the values of $\log(K_{sp})$ are -9.8, -12.3 and -16.0 respectively.[35]

$$AgX\,(s) \overset{K_{sp}}{\rightleftharpoons} Ag^+\,(aq) + X^-\,(aq) \quad (8),$$

$$K_{sp} = (a_{Ag^+})(a_{X^-}) = (\gamma_{Ag^+}[Ag^+])(\gamma_{X^-}[X^-]) \quad (9),$$

where a_j and γ_j are the activity and activity coefficient of species j respectively. The square brackets designate the concentrations of the relevant species. Assuming $\gamma = 1$ for both Ag^+ and X^-, K_{sp} can be approximated:

$$K_{sp} \cong [Ag^+][X^-] \quad (10),$$

The inlay in Figure 5 shows that the peak potential of the anodic stripping of AgNPs in KX electrolytes increases linearly with $\log(K_{sp})$ of the AgX products, suggesting the dependence of the peak position on the thermodynamic properties of the oxidation process. The peak of this oxidative stripping wave varies in a near Nernstian manner shifting ~57mV per decade in $\log(K_{sp})$.

In addition, the oxidation of AgNPs in the presence of any halide ions gives rise to a much sharper anodic stripping peak than in KNO_3 or deionized water, similar to the results discussed before in Section 3.3.1 (Figure 2). The sharper peak suggests the faster rate of oxidation of the AgNPs in the presence of halides. The difference in the rates of AgNPs oxidation in the presence of different halides cannot be determined from the anodic stripping voltammetry alone. Accordingly, the nano-impacts of AgNPs are studied in the presence of different anions, the results of which will yield the physical insights into the oxidation of silver at the electrode interface.

This article is protected by copyright. All rights reserved.

Accepted Manuscript

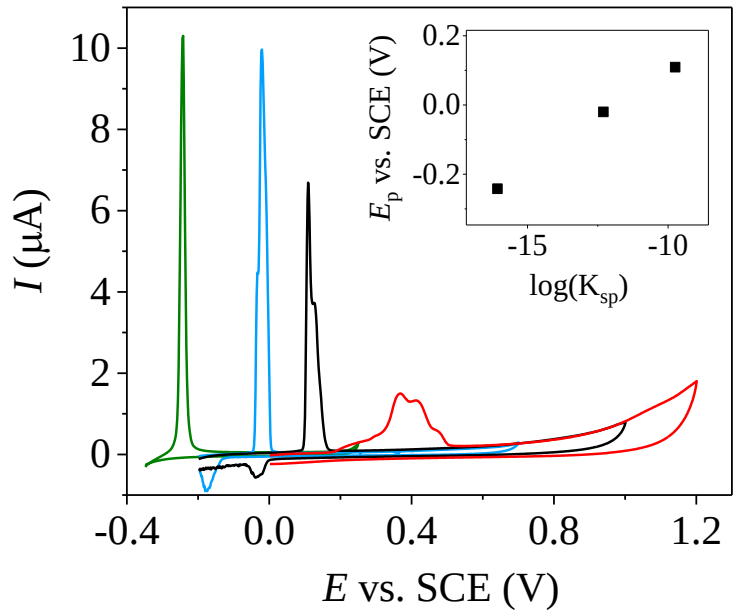

Figure 5: Anodic stripping of 2.4×10^{-16} moles of AgNPs dropcasted on a 3 mm diameter glassy carbon electrodes (surface coverage of 4.5%) in 20 mM of KNO_3 (red), KCl (black), KBr (blue) and KI (green); scan rate 10 mV s^{-1}. The inlay shows the peak potentials of AgNPs oxidation in different electrolytes plotted against the logarithm of the solubility constant ($\log(K_{sp})$) of AgX, where X is the different anions studied. The position of the oxidation peak in the presence of halides varies with ~57 mV per decade in $\log(K_{sp})$.

3.4.2 Nano-impacts: single nanoparticle collisions

Having evidenced the difference in the stripping potentials of AgNPs in the absence and presence of different electrolytes, next we investigate the nano-impact responses of AgNPs in 20 mM of KNO_3, KCl, KBr and KI. The suspensions of 12 pM AgNPs in 20 mM of varied electrolytes were subjected to cyclic voltammetry measurements at a carbon microdisc electrode at the scan rate of 10 mV s^{-1}.

For KNO_3 and KCl, the potentials were swept from 0 V to 1.2 V and back to 0 V vs. SCE. In the case of KBr and KI, the maximum potentials are limited to 0.7 V and 0.22 V vs. SCE respectively due to the oxidation of Br^- and I^- at higher potentials, and the nano-impact spikes would be masked by the oxidative responses of Br^- and I^-. More importantly, any Br_2 (E^0 = 1.06 V vs. SHE) or I_2 (E^0 = 0.54 V vs. SHE) formed would likely spontaneously oxidize the silver nanoparticles (E^0 = 0.07 and -0.15 V vs. SHE for oxidation to AgBr and AgI respectively),[28] decreasing the number of AgNPs available for the nano-impact measurements and hence result in the underestimation of the frequency of spikes.

This article is protected by copyright. All rights reserved.

Accepted Manuscript

10.1002/chem.201703591

Figure 6 presents the representative cyclic voltammograms showing nano-impact spikes of AgNPs oxidation in 20 mM of KNO_3 (Figure 6a), KCl (Figure 6b), KBr (Figure 6c) and KI (Figure 6d).

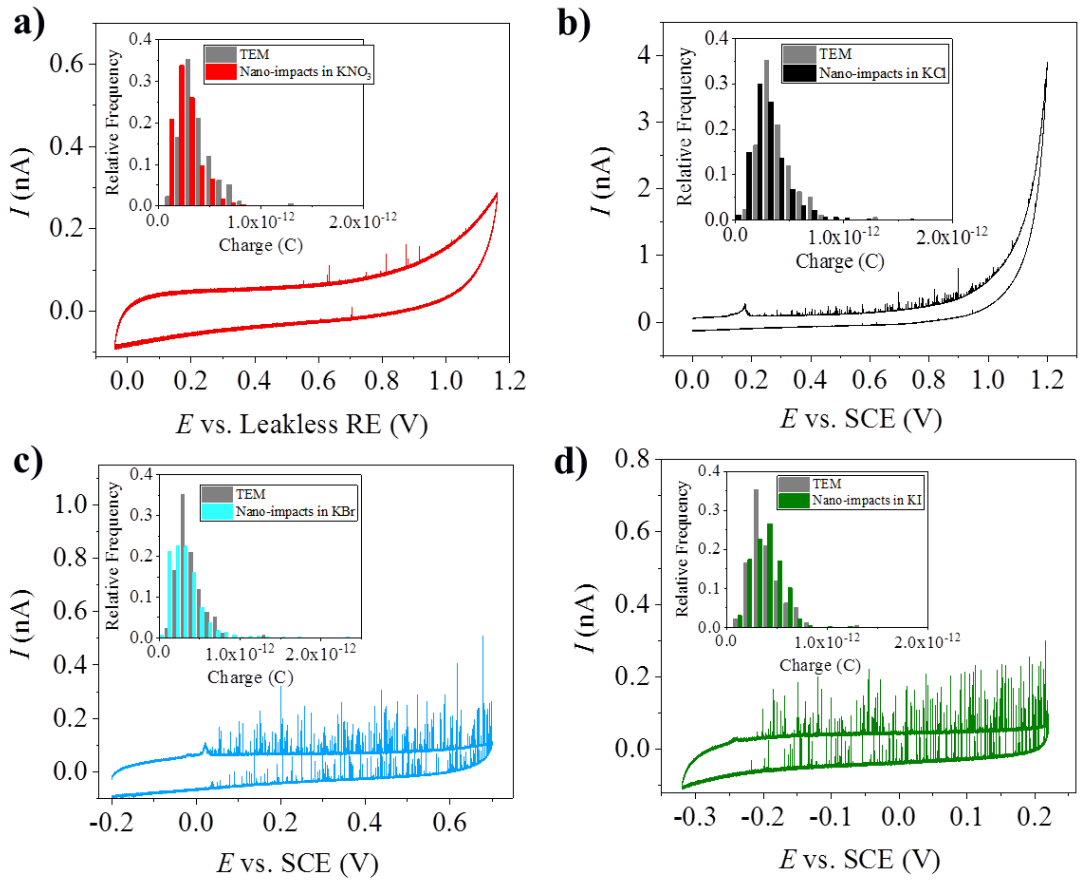

Figure 6: Representative cyclic voltammograms showing nano-impact spikes of 12 pM AgNPs in 20 mM of **a)** KNO_3; **b)** KCl; **c)** KBr; **d)** KI. The inlays display the distribution of AgNPs sizes calculated from the charge transfer of nano-impact spikes compared with the sizes determined using TEM. Carbon microdisc (20.5 µm radius) working electrode. Scan rate of 10 mV s^{-1}.

Also observable in these voltammograms are small stripping peaks associated with the oxidation of nanoparticles that have accumulated at the electrode between experiments. The position of these stripping peaks as a function of the anion identity is in excellent agreement with the results obtained from the drop-cast experiments (Figure 5). In stripping experiments the finite nature of the amount of material initially present on the electrode leads to the voltamemtric oxidation event only occurring at low electrode potentials. For a given salt no spikes are observed at potentials less positive than the stripping peak potentials. Moreover, the spikes are observed to onset at only tens of millivolts beyond the stripping peak. This delayed onset is consistent with being due to the relatively slow oxidation of the nanoparticle

This article is protected by copyright. All rights reserved.

Accepted Manuscript

(after initiation of the process) at low overpotentials, such an interpretation is consistent with the results presented by Tschulik.[15b] The amount of charge transferred is determined from the area under the spikes. The average and distribution of charges determined via nano-impact measurement is in excellent agreement with TEM, see histograms in the inlays of Figures 6a, 6b, 6c and 6d for the nano-impacts taking place in KNO_3, KCl, KBr and KI respectively. The charges transferred are in the order of $3.2 \times 10^{-13} \pm 1.8 \times 10^{-13}$ C for all the electrolytes at all the potentials above the stripping potentials (see SI section 10 for details). This corresponds to >80% of the expected charge as determined from the detailed TEM analysis (conservatively estimated as $Q_{equiv} = 3.9 \times 10^{-13} \pm 1.6 \times 10^{-13}$ C). However, due to the ambiguity associated with obtaining a volume from a 2D image, the bias of nano-imapct experiments towards the detection of smaller nanoparticles (due to their higher associated diffusion coefficient),[36] the insensitivity of the magnitude of this charge to the applied potential and the identity of the electrolyte, it is concluded that the data – within the accuracy of the presented work – is *fully consistent with* arising from the complete oxidation of the silver nanoparticles at the electrode surface. Hence, once the AgNPs reach a sufficiently biased electrode, they are completely oxidized. In terms of nanoparticle sizing any error in the volume measurement is minimised when converted to that of a length scale. From the charge histograms, we have further shown that not only the average value, but nano-impacts also provide an accurate determination of the size distribution (standard deviation) of the nanoparticles, in excellent agreement with TEM measurements (see Figure 4 a and the inlays of Figure 6 a-d).

A number of independent studies, including the present work, report the *complete* oxidation of the AgNPs upon the impact at a sufficiently biased electrode.[8, 15b, 19, 29] Meanwhile, the incomplete oxidation is reported in some cases, in particular for particles of larger sizes.[23a, b] In both cases these experiments were performed using a nitrate based electrolyte and, as evidenced above, this may *not* be the optimal conditions under which to study oxidative silver nanoparticle impacts. Furthermore, as discussed in Section 3.1 for relatively large nanoparticles (d > 20 nm), the shape of the AgNPs deviates from that of a sphere and the volume estimated from the two-dimensional TEM images is significantly lower than the circumscribed sphere. This missing volume of the particles may partially be the origin of the discrepancy in the sizes of AgNPs obtained from the nano-impact and TEM measurements reported in some cases. In this respect the work of Oja *et al.*is of distinct interest,[23b] notably they report only *qualitatively* similar results between experiments performed at two different

This article is protected by copyright. All rights reserved.

Accepted Manuscript

universities, using different equipment and different nanoparticles. Their SI seems to shows data where cf. 60% (University of Utah) of the nanoparticle material is accounted for in the electrochemical data (compared with the 25% (University of Washington) reported in the main text) and that the measured charge is seemingly sensitive to the systems filtering. We comment that this 'missing' ~40% may *plausibly* be fully accounted for if the non-sphericity of the particles is taken into account; however, the information provided in the article is insufficient for this conclusion to be definitively made. Quantitative discrepancies between different groups need to be accounted for.

In the present work, were the nanoparticles to undergo only partial oxidation one would anticipate a significant discrepancy between the measured and expected charge (as estimated by microscopy); moreover, the frequency of the impact events would be anticipated to be more than is observed experimentally due to the possibility of each particle undergoing multiple oxidative events. Aside from the subtleties of estimating particle volumes from 2D images, another possible reason of the discrepancy in the apparent 'completeness' of the AgNP oxidation event may relate to the difference in the bandwidth, sampling frequency and/or the associated transfer function[22, 37] of the electronics used for the measurement. Notably, some work in the literature[23a] does not provide sufficient information on the transfer function of the systems filtering to enable confirmation that the equipment used likely conserves the charge passed during an oxidation event. Interestingly the use of faster electronics allows the investigations of the dynamics of the AgNP oxidation.[15b, 23a, b] This in itself however may lead to the underestimation of the area (charge) of the spikes if the sampling rate is not sufficiently fast[38] or if inappropriate electronic filtering has been used. The utilisation of higher frequency bandwidths comes at the expense of higher noise, where lower current events may be masked by the associated larger background. In the case of using faster electronics which begin to resolve the oxidative events as multiple features, it is imperative to ensure that none of the charge associated with an oxidation is effectively 'lost' due to the associated poorer signal-to-noise ratio. Finally, we comment that for higher frequency measurements it becomes increasingly difficult to declare which groups of spikes correspond to the oxidation of the same AgNP, recognizing that the duration between individual stochastic events should follow a Poisson distribution. The use of lower bandwidth is neutral in respect to this last issue but partially side steps the problem by providing an effective but essentially arbitrary time threshold below which current is implicitly assumed to arise from the same event. Charge analysis in this work is done by assuming that an oxidative

This article is protected by copyright. All rights reserved.

Accepted Manuscript

feature ends when the current returns to the baseline i.e. any single feature may have multiple peaks, although as shown in the inlays of Figure 3 a-f, for the used filtering (100Hz analog two cascaded RCs, followed by a 100 Hz 4-pole Bessel digital filter post signal digitisation) the majority of spikes are seen to exhibit a single maxima and approximately correspond to the impulse response of the system.

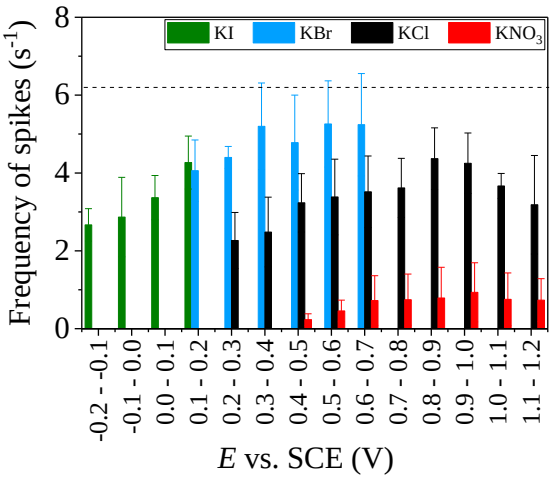

Figure 7: The bar graph showing the frequency of nano-impact spikes of AgNPs oxidation events. The dash line marks the diffusion-limited frequency of 6.2 s^{-1} predicted for the collisions of 12 pM AgNPs with a 20.5 µm radius microdisc electrode, using the AgNPs circumscribed radius of 24 nm. The different colours of the bar graphs designate the nano-impact of AgNPs in 20 mM of different supporting electrolytes: (green) KI, (blue) KBr, (black) KCl and (red) KNO_3.

In addition to the size of the nanoparticles, the frequency of nano-impact spikes is next evaluated. Figure 7 presents the resulting frequencies in different electrolytes at varied potentials. In the presence of Cl^-, Br^- or I^-, the frequencies of the collision events are significantly higher than in KNO_3, and the frequency increases with increasing potentials. These differences in frequencies are discussed in detail in the next section.

4 Discussion

The results of the nano-impact studies presented in Sections 3.3.2 and 3.4.2 will be discussed in detail in this section to gain insight into the oxidative mechanisms of AgNPs oxidation. The frequency of the nano-impact spikes may be governed by three parameters including the flux of the nanoparticles to the electrode, the quality and time of electrical contact between

This article is protected by copyright. All rights reserved.

Accepted Manuscript

the electrode and the nanoparticles, and the participation of the anions. Each point is discussed below.

First, there are three possible means of mass transport of the particles to the electrode: diffusion, migration and convection. Convection is assumed to be negligible as the oxidation of the AgNPs passes only a small current such that no significant temperature or density gradient is built up.[39] Migration is also unlikely to be a dominant factor as the change in the concentration of charged species at the electrode surface is very small as, for a single collision event, only one AgNP is oxidized releasing ~5.3 attomoles of Ag. Figure S6 in the SI also shows the similar surface charges (zeta-potentials) of the AgNPs in different electrolytes. Hence any electrostatic interaction such as the interaction between the electric double layer of the electrode and the Fermi level of the nanoparticle[40] are expected to be similar in all the electrolytes studied herein. The most important and relevant path of mass transport in this work is thus diffusion.

For nanoparticles moving freely in solution by Brownian motion, the diffusion-limited flux (J) of the nanoparticles to a microdisc electrode is expressed by the Shoup-Szabo equation:[41]

$$J = 4Dcr_{\mathrm{e}}f(\tau) \qquad (11),$$

where c is the particle number concentration (particles m^{-3}), r_{e} is the radius of the microdisc electrode.

$$f(\tau) = 0.7854 + 0.8862\tau^{-1/2} + 0.2146e^{\left(0.7823\tau^{-1/2}\right)} \qquad (12),$$

τ is the dimensionless time;

$$\tau = \frac{4Dt}{r_{\mathrm{e}}^2} \qquad (13),$$

t is the time parameter. D is the diffusion coefficient of the nanoparticle which can be estimated by the Stokes-Einstein equation:[42]

$$D = \frac{k_B T}{6\pi\eta r_{NP}} \qquad (14),$$

where k_B is the Boltzmann constant, T is the absolute temperature, η is the viscosity of solvent and r_{NP} is the radius of the nanoparticle.

This article is protected by copyright. All rights reserved.

Accepted Manuscript

The carbon microdisc electrode is made of a carbon microfiber surrounded with an insulating glass sheath of 2 mm radius. In the extreme case where all the AgNPs that reach the glass sheath stick to its surface, the flux of the AgNPs to the electroactive disc surface (J^S) is reduced to:[43]

$$J^S = J\frac{r_e}{2r_s} \quad (15),$$

Where r_e is the radius of the microdisc electrode, r_s is the radius of the insulating glass sheath, and J is the flux described in equation (11).

The carbon microdisc electrode used in this work has been characterized using the well-defined ruthenium hexamine ($[Ru(NH_3)_6]^{3+}/[Ru(NH_3)_6]^{2+}$) redox system[44] to have the disc radius (r_e) of 20.5 ± 0.1 μm; refer to Section S6 (SI). The insulating glass sheath radius (r_s) is 2.0 mm.

The sizes of AgNPs in 20 mM of KNO_3, KCl, KBr and KI have been demonstrated in Section 3.2 to be the same in all electrolytes throughout the entire period of the experiments (≤ 20 min). The viscosities of aqueous solutions containing 20 mM of salts are less than 0.04% higher than that of pure water (890.3 μPa s).[45] Consequently, the diffusion coefficients (D) are approximated to be ca. $1.1\times10^{-11} \pm 1.2\times10^{-12}$ m^2 s^{-1} using the AgNP (circumscribed) radius of 24 ± 3 nm of the AgNPs. In solution, the solvation of AgNPs has to be considered. The hydrodynamic radius of the AgNPs is determined using dynamic light scattering (DLS z-average) to be 30 ± 6 nm; see Section S7 (SI). Based on the hydrodynamic radius, the diffusion coefficients is $8.2\times10^{-12} \pm 1.3\times10^{-12}$ m^2 s^{-1}.

The diffusion-limited fluxes are calculated according to equation (11) to be 6.2 ± 0.7 s^{-1} and 4.9 ± 0.8 s^{-1} using the core and hydrodynamic radius respectively. The fluxes accounting for the 100% adsorption of the AgNPs on the insulating sheath calculated according to equation (15) are 0.032 ± 0.004 s^{-1} and 0.025 ± 0.004 s^{-1} using the core and hydrodynamic radius respectively.

From the results presented in Figure 7, the nano-impacts of AgNPs in 20 mM KBr at very high potentials yield the frequency of spikes of 5.2 ± 1.3 s^{-1}, close to the expected diffusional limit (within experimental error) of ca. 5 s^{-1}. However for most other cases (Figures 4b and

This article is protected by copyright. All rights reserved.

Accepted Manuscript

7), the observed spike frequencies are apparently lower than the predicted diffusion-limited value, up to an order of magnitude lower for KNO_3 and KCl at the low 5 mM concentration.

In Section S8 (SI), we demonstrate that less than 20% of the AgNPs that arrive at the glass surface are adsorbed, and that there is no difference in the adsorption rate between the AgNPs in KNO_3 and in KCl solutions. The observed frequencies are also significantly higher than that predicted for the case of full adsorption of AgNPs on the insulating glass sheath. Consequently, it is unlikely that the lower frequency observed is due to the loss of the material to the surrounding environments such as the insulating glass sheath around the electrode and the container. The lower frequency thus suggests that not every AgNP arriving at the electrode surface is oxidized. It is useful to reflect that for other experimental setups reported in the literature a variation in the frequency of the observed spikes as a function of the electrode potential has been reported.[46] However, for the present case it is challenging to interpret the variation of the nano-particle impact frequency, as a function of the anion identity, as relating to changes in the nanoparticle mass-transport. Consequently, in light of the results discussed above that the difference in the frequencies of nanoparticle-electrode collisions is *not* a result of the difference in the flux of the AgNPs to the electrode.

Next, we consider the quality and the timescale of the electrical contact between the particles and the electrode. In terms of the charges of the nanoparticles, the surface charges are similar between AgNPs in KNO_3 and KCl, as discussed above. The equal surface charges measured in both KNO_3 and KCl solutions also suggest that no modification is made to the surface of the AgNPs, and that citrate ions may remain as capping agents. Therefore, there should be no difference in the quality and time of contacts.

The difference in the frequency must then arise from the involvement of the anions in the oxidation of AgNPs, in particular during its rate-determining process. The lower frequency in the case of KNO_3 suggests that not all of the AgNPs that arrive at the electrode have been oxidized, implying that the rate at which the AgNPs are oxidized is slower than the time the AgNPs stay at the electrode. The higher frequency of the nano-impact spikes in potassium halide solutions suggests that the halide ions (X^-) accelerate the rate-determining process of the AgNPs oxidation. This altered mechanism is also in part reflected in the altered shape of the voltammetric stripping wave (Figure 5). The processes that involve anions are the diffusion of X^- *to* the AgNPs, the diffusion of X^- *into* the AgNPs, and the nucleation and growth of AgX.

This article is protected by copyright. All rights reserved.

Accepted Manuscript

It is shown in Figure 7 that the frequency of the collision events is not distinctly different (within experimental errors) between the different halides. If any, the frequency in the presence of Cl^- is lower than that of Br^- and I^-. Consequently, we infer that the diffusion of X^- to the AgNPs is *not* the rate-determining step of the AgNPs oxidation as the diffusion coefficients of the ions follow the opposite order. The diffusion of X^- into AgNPs or the propagation of the formation of Ag(I) products from the surface into the core of the particles is also *not* a possible initial rate-determining process as once the AgNP is oxidized, the reaction goes to completion (Figure 4a and Inlays in Figure 6). The use of faster electronics may resolve the kinetics of this growth stage.

In the light of the above – and partially in analogy to pitting corrosion[47] – we propose that the AgNP oxidation follows a nucleation growth type mechanism such that the observation of an oxidation event is preceded by the stochastic formation of a nucleus of argentous species (Ag^+, AgCl, AgBr or AgI). This initial oxidation event must occur during electrical contact of the nanoparticle to the electrode surface. Accordingly, the sensitivity of the impact frequency towards the nature and concentration of the supporting electrolyte anions reflects the altered rate of this stochastic process. The higher formation constants for the halide/Ag+ complexes likely make the initiation process more favourable. This rate of initial nucleation may well be sensitive to the faceting and local surface structure of individual particles.[48] After initiation, the subsequent rates of the nanoparticle oxidation, as reflected in the resulting spike shapes, may either arise from the nanoscale growth and dissolution of the material or alternately may relate to the nanoscopic motion of the nanoparticle (and hence its electrical connectivity) adjacent to the electrochemical interface.

5 Conclusions

The ability of the nano-impact technique to investigate the relative kinetics of nanoparticle oxidative dissolution is demonstrated in this work, by comparing the rate of the oxidation to the timescale the particles remain in electrical contact with the electrode and hence the frequency of spikes. The frequency is influenced by the electrolyte's identity and concentrations as well as the applied potentials. In the presence of anions that bind strongly to the oxidation product such as Ag(I) in the oxidative dissolution of AgNPs, the thermodynamically favourable product formation shifts the anodic stripping peaks to more negative potentials and enhance the frequency of spikes. Notably, we observed the *complete*

This article is protected by copyright. All rights reserved.

Accepted Manuscript

oxidation of the AgNP upon impacting at a sufficiently biased electrode. The importance of rigorous evaluation of the particle volume from two-dimensional transmission electron microscope (TEM) images is emphasized. Exact determination of a nanoparticle volume from a 2D image is not possible, leading to ambiguity in the sizing. This is particularly important when the TEM size is required for comparison with techniques which yield the atomic content of the particles as opposed to the length scale. In the nano-impact measurements, the total charge transferred under each spike is *not* influenced by the electrolyte nor the potential applied at the working electrode. On this basis, we gain physical insights into the oxidation of AgNPs at the electrode surface and reveal that the rate-determining process is the formation of the first oxidized Ag(I) products (similar to pit initiation). The fundamental understanding of this process facilitates the choice of electrolytes in various applications. For example, the determination of the size of AgNPs at low electrolyte concentrations can be achieved by nano-impact measurements at any high over-potential in the presence of e.g. 1 mM of Cl^-, the concentration of which is present in natural river and drinking water.

Acknowledgements

KN receives funding from the Royal Thai government under the DPST scholarship program. This project is supported by the funding from the European Research Council under the European Union's Seventh Framework Programme (FP/2007-2013)/ERC Grant Agreement no. [320403].

Supporting Information

TEM imaging of AgNPs; Contamination of Cl^- from standard calomel reference electrode; Stability of the AgNPs in different electrolytes; Nano-impacts of AgNPs in deionized water; Zeta-potentials of AgNPs; Characterization of the carbon microdisc electrode; Hydrodynamic sizes of AgNPs; Adsorption of AgNPs on a glass surface.

References

[1] a) R. W. Murray, *Chem. Rev.* **2008**, *108*, 2688-2720; b) A. Economou, D. W. M. Arrigan, J. Campo, S. M. Reddy, S. Lunte, M. Thompson, C. Kranz, R. G. Compton, A. O'Riordan and C. E. Banks, *Electrochemical Strategies in Detection Science (Chapter 5)*, Royal Society of Chemistry, **2015**, p.
[2] a) T. R. Copeland and R. K. Skogerboe, *Anal. Chem.* **1974**, *46*, 1257A-1268a; b) W. D. Ellis, *J. Chem. Educ.* **1973**, *50*, A131.

This article is protected by copyright. All rights reserved.

Accepted Manuscript

[3] K. Tschulik, K. Ngamchuea, C. Ziegler, M. G. Beier, C. Damm, A. Eychmueller and R. G. Compton, *Adv. Func. Mat.* **2015**, *25*, 5149-5158.
[4] B. J. Plowman, B. Sidhureddy, S. V. Sokolov, N. P. Young, A. Chen and R. G. Compton, *ChemElectroChem* **2016**, *3*, 1186-1186.
[5] C. C. M. Neumann, C. Batchelor-McAuley, K. Tschulik, H. S. Toh, P. Shumbula, J. Pillay, R. Tshikhudo and R. G. Compton, *ChemElectroChem* **2014**, *1*, 87-89.
[6] H. S. Toh, C. Batchelor-McAuley, K. Tschulik, M. Uhlemann, A. Crossley and R. G. Compton, *Nanoscale* **2013**, *5*, 4884-4893.
[7] a) S. J. Cloake, H. S. Toh, P. T. Lee, C. Salter, C. Johnston and R. G. Compton, *ChemistryOpen* **2015**, *4*, 22-26; b) S. E. Ward Jones, F. W. Campbell, R. Baron, L. Xiao and R. G. Compton, *J. Phys. Chem. C* **2008**, *112*, 17820-17827.
[8] H. S. Toh, K. Jurkschat and R. G. Compton, *Chem Eur. J.* **2015**, *21*, 2998-3004.
[9] X. Dai and R. G. Compton, *Electroanalysis* **2005**, *17*, 1325-1330.
[10] a) O. S. Ivanova and F. P. Zamborini, *J. Am. Chem. Soc.* **2010**, *132*, 70-72; b) M. Giovanni and M. Pumera, *Electroanalysis* **2012**, *24*, 615-617.
[11] a) S. V. Sokolov, S. Eloul, E. Katelhon, C. Batchelor-McAuley and R. G. Compton, *Phys. Chem. Chem. Phys.* **2016**, *19*, 28-43; b) W. Cheng and R. G. Compton, *TrAC, Trends Anal. Chem.* **2014**, *58*, 79-89; c) M. Pumera, *ACS nano* **2014**, *8*, 7555-7558.
[12] S. V. Sokolov, T. R. Bartlett, P. Fair, S. Fletcher and R. G. Compton, *Anal. Chem.* **2016**, *88*, 8908-8912.
[13] a) L. J. Zhao, R. C. Qian, W. Ma, H. Tian and Y. T. Long, *Anal. Chem.* **2016**, *88*, 8375-8379; b) Y. L. Ying, Z. Ding, D. Zhan and Y. T. Long, *Chem. Sci.* **2017**, *8*, 3338-3348; c) X. Zhou, W. Xu, G. Liu, D. Panda and P. Chen, *J. Am. Chem. Soc.* **2010**, *132*, 138-146; d) Z. Guo, S. J. Percival and B. Zhang, *J. Am. Chem. Soc.* **2014**, *136*, 8879-8882; e) X. Xiao and A. J. Bard, *J. Am. Chem. Soc.* **2007**, *129*, 9610-9612; f) A. J. Bard, H. Zhou and S. J. Kwon, *Israel J. Chem.* **2010**, *50*, 267-276.
[14] K. J. Stevenson and K. Tschulik, *Curr. Opin. Electrochem.* **2017**.
[15] a) B. Haddou, N. V. Rees and R. G. Compton, *Phys. Chem. Chem. Phys.* **2012**, *14*, 13612-13617; b) E. N. Saw, M. Kratz and K. Tschulik, *Nano Res.* **2017**.
[16] S. Eloul, E. Kätelhön, C. Batchelor-McAuley, K. Tschulik and R. G. Compton, *J. Electroanal. Chem.* **2015**, *755*, 136-142.
[17] K. J. Krause, F. Brings, J. Schnitker, E. Katelhon, P. Rinklin, D. Mayer, R. G. Compton, S. G. Lemay, A. Offenhausser and B. Wolfrum, *Chem Eur. J.* **2017**, *23*, 4638-4643.
[18] N. R. Panyala, E. M. Peña-Méndez and J. Havel, *J. App. Biomed.* **2008**, *6*.
[19] T. R. Bartlett, S. V. Sokolov, B. J. Plowman, N. P. Young and R. G. Compton, *Nanoscale* **2016**, *8*, 16177-16181.
[20] C. de Mello Donegá, *Nanoparticles: Workhorses of Nanoscience*, Springer Berlin Heidelberg, **2014**, p.
[21] C. Batchelor-McAuley, J. Ellison, K. Tschulik, P. L. Hurst, R. Boldt and R. G. Compton, *Analyst* **2015**, *140*, 5048-5054.
[22] E. Kätelhön, E. E. L. Tanner, C. Batchelor-McAuley and R. G. Compton, *Electrochim. Acta* **2016**, *199*, 297-304.
[23] a) J. Ustarroz, M. Kang, E. Bullions and P. R. Unwin, *Chem. Sci.* **2017**, *8*, 1841-1853; b) S. M. Oja, D. A. Robinson, N. J. Vitti, M. A. Edwards, Y. Liu, H. S. White and B. Zhang, *J. Am. Chem. Soc.* **2017**, *139*, 708-718; c) X. Li, J. J. Lenhart and H. W. Walker, *Langmuir* **2010**, *26*, 16690-16698; d) S. V. Sokolov, C. Batchelor-McAuley, K. Tschulik, S. Fletcher and R. G. Compton, *Chem Eur. J.* **2015**, *21*, 10741-10746.
[24] D. R. Lide, *CRC Handbook of Chemistry and Physics: A Ready-reference Book of Chemical and Physical Data*, CRC-Press, **1995**, p.
[25] R. Esteban, R. W. Taylor, J. J. Baumberg and J. Aizpurua, *Langmuir* **2012**, *28*, 8881-8890.
[26] H. S. Toh, C. Batchelor-McAuley, K. Tschulik and R. G. Compton, *Analyst* **2013**, *138*, 4292-4297.
[27] R. G. Compton and C. E. Banks, *Understanding Voltammetry*, Imperial College Press, **2011**, p. 444.
[28] A. J. Bard, R. Parsons and J. Jordan, *Standard Potentials in Aqueous Solution*, Taylor & Francis, **1985**, p.

This article is protected by copyright. All rights reserved.

Accepted Manuscript

[29] V. Brasiliense, A. N. Patel, A. Martinez-Marrades, J. Shi, Y. Chen, C. Combellas, G. Tessier and F. Kanoufi, *J. Am. Chem. Soc.* **2016**, *138*, 3478-3483.
[30] a) L. S. Y. Ly, C. Batchelor-Mcauley, K. Tschulik, E. Kätelhön and R. G. Compton, *J. Phys. Chem. C* **2014**, *118*, 17756-17763; b) Y. Liu, B. J. J. Austen, T. Cornwell, R. D. Tilbury, M. A. Buntine, A. P. O'Mullane and D. W. M. Arrigan, *Electrochem. Comm.* **2017**, *77*, 24-27.
[31] a) X. Li, C. Batchelor-Mcauley, S. A. I. Whitby, K. Tschulik, L. Shao and R. G. Compton, *Angew. Chem. Int. Ed.* **2016**, *55*, 4296-4299; b) S. J. Percival and B. Zhang, *J. Phys. Chem. C* **2016**, *120*, 20536-20546.
[32] H. Hodson, X. Li, C. Batchelor-Mcauley, L. Shao and R. G. Compton, *J. Phys. Chem. C* **2016**, *120*, 6281-6286.
[33] a) E. J. F. Dickinson, N. V. Rees and R. G. Compton, *Chem. Phys. Lett.* **2012**, *528*, 44-48; b) W. Ma, H. Ma, J. F. Chen, Y. Y. Peng, Z. Y. Yang, H. F. Wang, Y. L. Ying, H. Tian and Y. T. Long, *Chem. Sci.* **2017**, *8*, 1854-1861.
[34] a) J. Liu and R. H. Hurt, *Environ. Sci. Tech.* **2010**, *44*, 2169-2175; b) B. J. Plowman, K. Tschulik, E. Walport, N. P. Young and R. G. Compton, *Nanoscale* **2015**, *7*, 12361-12364.
[35] R. Alexander, E. C. F. Ko, Y. C. Mac and A. J. Parker, *J. Am. Chem. Soc.* **1967**, *89*, 3703-3712.
[36] J. C. Lees, J. Ellison, C. Batchelor-McAuley, K. Tschulik, C. Damm, D. Omanovic and R. G. Compton, *Chemphyschem* **2013**, *14*, 3895-3897.
[37] E. Kätelhön, A. Feng, W. Cheng, S. Eloul, C. Batchelor-McAuley and R. G. Compton, *J. Phys. Chem. C* **2016**, *120*, 17029-17034.
[38] Due to the charge passed during an oxidative event being of interest it is imperative that the sampling rate is at least an order of magnitude greater than the bandwidth of the filtering system (the present work oversamples at a factor of 500). The exact sampling rate required to ensure the shape and hence charge is accurately reported will be highly system dependent.
[39] K. Ngamchuea, S. Eloul, K. Tschulik and R. G. Compton, *Anal. Chem.* **2015**, *87*, 7226-7234.
[40] P. Peljo, J. A. Manzanares and H. H. Girault, *Chem. Sci.* **2017**, *8*, 4795-4803.
[41] D. Shoup and A. Szabo, *J. Electroanal. Chem.* **1982**, *140*, 237-245.
[42] a) W. Sutherland, *Philosophical Magazine Series 6* **1905**, *9*, 781-785; b) A. Einstein, *Annalen der Physik* **1905**, *322*, 549-560.
[43] S. Eloul and R. G. Compton, *ChemElectroChem* **2014**, *1*, 917-924.
[44] Y. Wang, J. G. Limon-Petersen and R. G. Compton, *J. Electroanal. Chem.* **2011**, *652*, 13-17.
[45] a) J. Kestin, M. Sokolov and W. A. Wakeham, *J. Phys. Chem. Ref. Data* **1978**, *7*, 941-948; b) Hai-Lang and Shi-Jun, *J. Chem. Eng. Data* **1996**, *41*, 516-520.
[46] a) A. N. Patel, A. Martinez-Marrades, V. Brasiliense, D. Koshelev, M. Besbes, R. Kuszelewicz, C. Combellas, G. Tessier and F. Kanoufi, *Nano Lett.* **2015**, *15*, 6454-6463; b) M. Kang, D. Perry, Y. R. Kim, A. W. Colburn, R. A. Lazenby and P. R. Unwin, *J. Am. Chem. Soc.* **2015**, *137*, 10902-10905.
[47] G. T. Burstein, C. Liu, R. M. Souto and S. P. Vines, *Corro. Eng. Sci. Tech.* **2013**, *39*, 25-30.
[48] However, we comment that in the the present work there is no evidence for a significant difference - as a function of the electrolyte concentration and identity - in the electrochemically measured particle size (charge) distribution.

Accepted Manuscript

This article is protected by copyright. All rights reserved.

10.1002/chem.201703591

Table of Contents

Single silver nanoparticle (AgNP) detection: Nano-impacts or single nanoparticle-electrode collisions allow the detection of *individual* nanoparticles. Upon the impact, AgNP undergoes *complete* oxidation. The technique further allows the rate-determining process of silver oxidation at the electrode interface to be determined.

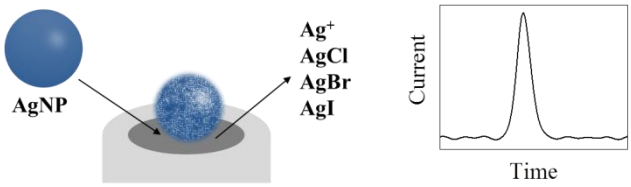

This article is protected by copyright. All rights reserved.

Accepted Manuscript